Limits on Spin-Mass Couplings within the Axion Window

A. N. Youdin, D. Krause, Jr., K. Jagannathan, and L. R. Hunter
Physics Department, Amherst College, Amherst, Massachusetts 01002

S. K. Lamoreaux
Physics Department, University of Washington, Seattle, Washington 98195
(Received 10 June 1996)

We compare the relative precession frequencies of Hg and Cs magnetometers as a function of the position of two 475 kg lead masses with respect to an applied magnetic field. Our observations limit the size of a possible monopole-dipole interaction expected to be produced by a pseudoscalar particle such as the axion. For a range of 20 cm, the products of the scalar and pseudoscalar couplings ($g_s g_p/\hbar c$) are found to be less than 2.3×10^{-29} and 3.6×10^{-29} for couplings to the electron and neutron spins, respectively. The e (n) limits are approximately 3 (4) orders of magnitude better than earlier experiments. [S0031-9007(96)01097-6]

PACS numbers: 14.80.Mz, 32.80.Bx, 34.20.Cf

Axions are well known as an elegant solution to the strong CP problem as well as an interesting dark-matter candidate [1]. One of the most remarkable and least explored predictions associated with the axion is that it would yield a parity and time-reversal violating, monopole-dipole coupling between spin and matter of the form [2]

$$V = \hbar(g_s g_p)\frac{\sigma \cdot \hat{\mathbf{r}}}{8\pi m_p c}\left(\frac{1}{\lambda r} + \frac{1}{r^2}\right)e^{-r/\lambda}, \qquad (1)$$

where V is the two-fermion interaction potential, $\sigma\hbar/2$ is the fermion spin, $\mathbf{r}$ is the displacement vector between the mass and the spin, g_p and g_s are the coupling constants at the vertices of the polarized and unpolarized particles, respectively, and m_p is the mass of the polarized particle. Experimental and astrophysical observations imply that the mass of the axion must lie between 1 μeV and 1 meV, corresponding to a range, λ, between 20 cm and 0.2 mm [3]. This range is commonly referred to as the "axion window."

For ranges larger than about a meter, good experimental limits on the product $g_s g_p$ are obtained from experiments that search for a coupling between either Be^+ or ^{199}Hg and the Earth [4,5]. A torsion-pendulum experiment explicitly establishes limits on the product $g_s g_p$ in the axion window, but is only sensitive to terms involving electron spin [6]. As we shall see in the theoretical analysis, nuclear spin provides a more sensitive and more model-independent probe for possible axion couplings.

To search for this axion coupling, we compare the precession frequencies of atomic ^{199}Hg and Cs when a large mass is positioned near the cells, relative to an applied magnetic field $\mathbf{B}$. The monopole-dipole potential described in Eq. (1), when integrated over the mass distribution, produces a frequency splitting K between adjacent magnetic sublevels of the atomic ground state. The total atomic precession frequency (including the magnetic and monopole-dipole coupling) can then be written for each atom as $f = \gamma B \pm K \equiv \gamma B^{\text{eff}}$, where $\gamma_{\text{Cs}} = 350$ kHz/G and $\gamma_{\text{Hg}} = 759$ Hz/G are the atomic ground-state gyromagnetic ratios and the $(+)$ or $(-)$ sign depends on the relative position of the mass with respect to $\mathbf{B}$. The difference between the effective magnetic fields, B^{eff}, measured by the Cs and Hg oscillators, is

$$\Delta B^{\text{eff}} = B^{\text{eff}}_{\text{Cs}} - B^{\text{eff}}_{\text{Hg}} = \pm\left(\frac{K_{\text{Cs}}}{\gamma_{\text{Cs}}} - \frac{K_{\text{Hg}}}{\gamma_{\text{Hg}}}\right). \qquad (2)$$

^{199}Hg is sensitive to only nuclear spin while Cs is predominantly sensitive to electron spin couplings. A comparison of the two systems thus allows us to cancel fluctuations in the ambient magnetic field while simultaneously retaining a sensitivity to both nuclear and electron spin couplings. For axionlike couplings we shall see that the K/γ ratio is much larger for Hg than for Cs, so that an "accidental" cancellation of the two terms is not likely.

The operation of the magnetometers and much of the experimental apparatus is similar to that previously described in a search for a violation of local Lorentz invariance [7]. A schematic of the key new elements of the experiment is shown in Fig. 1. A single Cs resonance cell is sandwiched between two Hg cells and the cell stack is oriented with its symmetry axis in the horizontal plane (along $\hat{\mathbf{j}}$). The cells are mounted in the center of three concentric cylindrical magnetic shields with their symmetry axis along $\hat{\mathbf{i}}$. The 894 nm (254 nm) radiation for the light absorption oscillators travels along $\hat{\mathbf{i}}$ $(-\hat{\mathbf{i}})$ for the Cs (Hg) magnetometers. The fixed magnetic field is oriented such that $\mathbf{B} = \pm B(-\hat{\mathbf{i}} + \hat{\mathbf{j}})/\sqrt{2}$, where the $(+)$ or $(-)$ correspond to the two opposing directions of the 5.3 mG magnetic field. An oscillating magnetic field, modulating near the Larmor frequencies of the two atoms, is applied along the vertical axis ($\hat{\mathbf{k}}$). The modulation frequencies are $f = \omega/2\pi = 4.0321$ Hz and 1.858 kHz for the Hg and Cs magnetometers, respectively. The cells, light sources, magnetic field locking, and detection electronics are all identical to those described in Ref. [7].

 0031-9007/96/77(11)/2170(4)$10.00

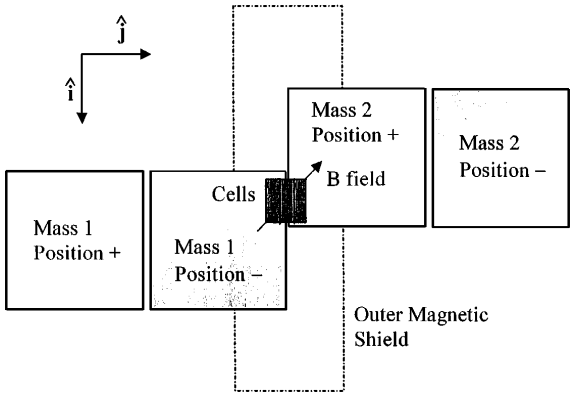

FIG. 1. The experimental geometry, showing the two positions of the two 475 kg lead masses, the three magnetometer cells, and the direction of the fixed magnetic field **B**. The lead blocks wrap halfway around the cylindrical magnetic shields. The figure is not to scale.

The spin relaxation times are about 30 s for the Hg atoms and 30 ms for the Cs atoms.

The most important new element of the apparatus is the assembly that allows two 475 kg lead masses to be moved around the magnetic resonance cells. Each of the lead blocks is a cube with 38 cm sides, and a 15 cm radius semicylindrical cutaway that allows the blocks to fit snugly around (but not touch) the magnetic shields. The two blocks are suspended from a movable nonmagnetic track, which is itself suspended from the ceiling. The two blocks are on opposite sides of the apparatus and are displaced asymmetrically from the center line by 11 cm (along $\hat{\mathbf{i}}$) in order to maximize the expected value of K. The assembly allows one to alternate between having one or the other block snug up against the shields while the other is removed a distance of 40 cm from the shields. In this manner, the sign of $\mathbf{r}$, and hence K and ΔB^{eff}, can be easily reversed. Because the distant block is not removed to infinity, its presence reduces the mass dipole. For $\lambda = 20$ cm, the resulting reduction in sensitivity is less than 5%.

It is crucial that the magnetic field affecting the atoms should not be significantly modified upon moving the block assembly. When the lead blocks are poured, care is taken to ensure that the entire block remains in the liquid state for some time to allow ferromagnetic contaminants to float to the surface, where they are subsequently removed. The remainder of the mass-moving assembly is constructed entirely from aluminum and brass. The assembly is moved between its two rest positions by an ac driving motor in a remote corner of the room, connected to the apparatus by a nylon rope. No data are collected for 150 s after moving the blocks to be sure that the atoms have had several spin relaxation times to recover from any transient fields. A 3D fluxgate magnetometer (APS model 520A) is placed 31 cm below the cells, outside the magnetic shields in order to monitor changes in the magnetic field. The magnetic field outside the magnetic shields changes by less than 1 μG when the lead blocks are moved between their two rest positions. This field is reduced by at least a factor of 1000 by the shields. Finally, the effects of any homogeneous magnetic field or uniform magnetic gradient within the shields is removed by taking the difference between the effective fields experienced by the Hg and Cs magnetometers [see Eq. (2)].

Data are gathered by measuring the change in ΔB^{eff} for each of the two positions [$(+)$ or $(-)$] of the lead blocks and forming the average difference, $\Delta B = [(\Delta B^{\text{eff}})_+ - (\Delta B^{\text{eff}})_-]/2$. Taking the difference doubles our sensitivity and eliminates effects (such as magnetic inhomogeneities and imperfect frequency settings) which do not depend on the mass position. A data point is formed by calculating ΔB for sequential mass positions $(+--+) = M+$, or $(-++-) = M-$. In this way any uniform drifts in the signal are removed. A set of five data points is collected using the sequence $M+$, followed by another set of five data points collected using the sequence $M-$. The helicity of the Cs light is then reversed [from $(+)$ to $(-)$], and ten additional points are collected following the same pattern. Finally, the Hg helicity is reversed, and the entire sequence used for the first twenty points is repeated. At the beginning of each cycle of five data points, the atomic magnetometers are calibrated by the application of a well known homogeneous magnetic field, and the gradient of the magnetic field along the cells is adjusted. A complete cycling through all helicities and mass sequences requires the collection of forty data points and about 9.6 h of operation. Of the 9.6 h, only about 3.2 h are actually spent integrating the signal; the rest is spent calibrating, adjusting the gradient field, and waiting for the magnetometers to settle after a change in the experimental configuration.

Our total data sample consists of 775 data points collected on three successive weekends in April, 1996 [8]. Of the 775 data points, 6 are rejected using Chauvenet's criterion [9]. The rejected points are most likely associated with abrupt changes in the ambient local magnetic field during data collection. The remaining data are grouped into complete cycles of approximately 40 data points and are shown in Fig. 2. The direction of the fixed magnetic field is positive in runs 1 and 4 and negative in runs 2 and 3. Throughout this discussion, the sign is chosen such that positive ΔB corresponds to an increase (decrease) in the Cs (Hg) frequency when **B** points in the direction of the nearby mass. The average of all the data yields the value $\Delta B = 2 \pm 16$ pG. Table I shows the results of subdividing the data by various criteria. No statistically significant variations from the global mean are observed, suggesting that light shifts (which would produce different effects for different helicities) and electronics effects (which would produce opposing effects for the different directions of **B**) are unimportant. The data are consistent with a random distribution with a χ^2 of 19.6 for 19 degrees of freedom.

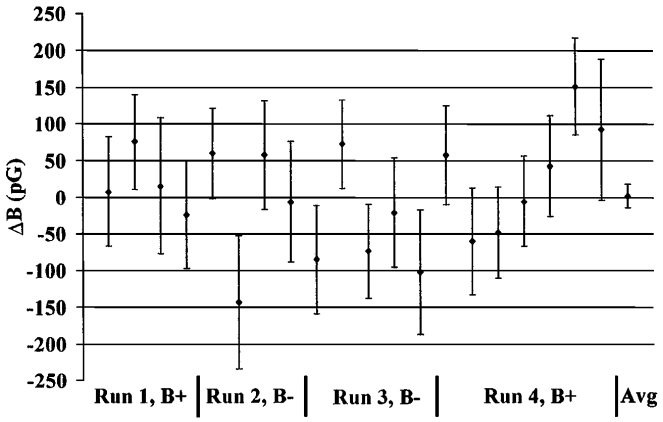

FIG. 2. ΔB as measured in blocks of about 40 data points. The direction of the fixed field **B** is indicated for each of the four data runs. The χ^2 is 19.6 for 19 degrees of freedom.

In addition to a possible systematic error associated with magnetic changes associated with the motion of the block assembly, discussed above, we have also considered the possibility that the shifting masses might produce a shift in the optical alignment of the magnetometers. Of greatest concern is the possibility that a small motion of the Cs beam in the presence of a magnetic field gradient could produce a change in the mean magnetic field that would be sampled by the Cs, but not by the Hg. A number of precautions have been taken to minimize this effect. First, suspension of the masses from the ceiling supresses the mechanical coupling between the mass position and the optical table, which is supported by the floor. In addition, a quadrant fiber assembly provides a feedback signal that is used to maintain a constant beam position, and the magnetic gradients are minimized using the algorithms outlined in Ref. [7]. With these additional precautions we believe that the effects associated with both beam motion and residual magnetization of the blocks are both less than 10% of our statistical uncertainty, and hence can be neglected when combined in quadrature.

TABLE I. The mean value of ΔB calculated using selected subsets of the data. N is the number of data points in each configuration.

Selection criteria	N	ΔB (pG)
B+	416	25(22)
B−	353	−25(25)
$\sigma_{\mathrm{Hg}}+$	399	−8(22)
$\sigma_{\mathrm{Hg}}-$	370	13(25)
$\sigma_{\mathrm{Cs}}+$	388	−9(24)
$\sigma_{\mathrm{Cs}}-$	381	14(23)
Run 1	160	19(38)
Run 2	155	−4(37)
Run 3	198	−41(32)
Run 4	256	29(26)
None	769	2(16)

We would like to relate our experimental result to limits on $g_s g_p$ for the neutron and electron. In a simple shell model, the ^{199}Hg valence nucleon is a $P_{1/2}$ state neutron; this implies that the neutron spin is $-1/3$ of the total nuclear spin [10]. Similarly, the electron-spin projection for Cs is $1/8$ of the total spin, $F = 4$, for the Cs ground state. This implies that $K_n = -3K_{\mathrm{Hg}}$ while $K_e = 8K_{\mathrm{Cs}}$. Finally, a numerical integration of Eq. (1) over the mass distribution for a variety of possible ranges allows us to relate our measurement of ΔB to the limits on the product $g_s g_p$ shown in Fig. 3, along with the limits established from other experiments. Note that the limits on the electron placed from Ref. [6] have been multiplied by $8\pi^2$ to correct an error in the earlier publication [11]. The limits from Ref. [4] are everywhere 1 order of magnitude less restrictive than those of Ref. [5] and have been omitted from the plot. For coupling to the electron spin, our results represent an improvement of about a factor of 1000 at the upper end of the axion range, while for coupling to the neutron spin, our results place the first significant constraints within the axion window.

To compare these results with what one would expect from the existence of an axion, we have extended the theory outlined in Ref. [2] for an electron-spin coupling to include possible effects associated with a coupling

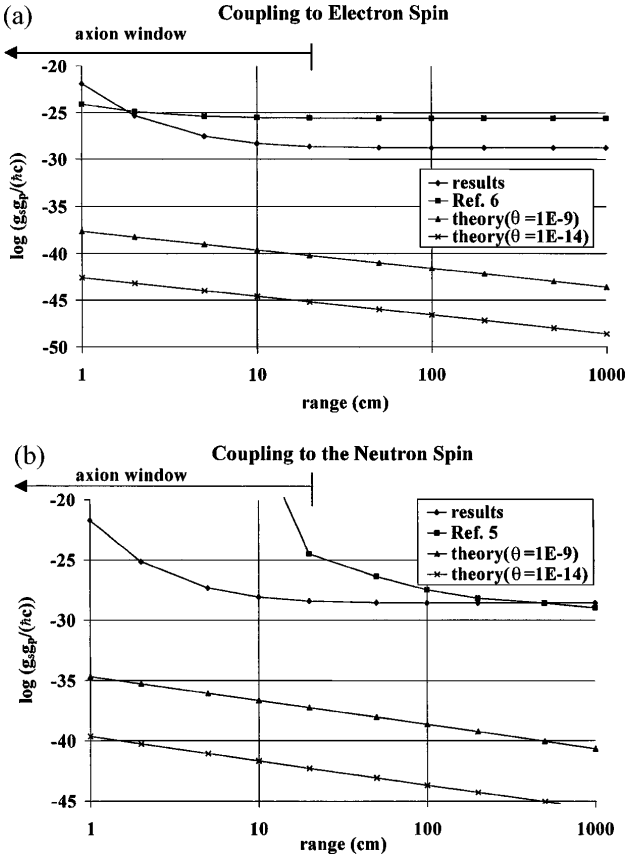

FIG. 3. Plots comparing the experimental upper bounds and theoretical predictions for the monopole-dipole couplings to (a) the electron spin and (b) the neutron spin.

to neutron spin. Following Ref. [1], the pseudoscalar coupling for the electron is given to first order by $(g_{aee})_p = X_e m_e / f_{\mathrm{PQ}}$, where f_{PQ} is the Peccei-Quinn symmetry-breaking scale, m_e is the electron mass, and X_e is the Peccei-Quinn charge for the electron, a model-dependent parameter that can take on values between 0 (in the hadronic model of the axion where there is no tree level coupling to leptons) and 1 (the value assumed in Ref. [2]). For neutrons, there are additional complications associated with the quark structure. The pseudoscalar coupling for the neutron can be written as

$$(g_{ann})_p = [(-F_{A0} + F_{A3})(X_u/2N - 0.32) + (-F_{A0} - F_{A3})(X_d/2N - 0.18)] \frac{m_n}{f_{\mathrm{PQ}}/N} \cong -0.08 \frac{m_n}{F_{\mathrm{PQ}}/N} \cong \frac{-450\ \mathrm{MeV}}{f_{\mathrm{PQ}}}.$$

Here $F_{A0} \approx -0.75$ and $F_{A3} \approx -1.25$ are the isoscalar and isovector parts of the axial vector pion-nucleon coupling while N is the model-dependent color anomaly of the Peccei-Quinn symmetry, taken to be 6. X_u and X_d are the Peccei-Quinn charges of the up and down quarks and are taken to be equal to 1. Following Ref. [2], we take the scalar coupling to nucleons to be

$$(g_{aNN})_s = \frac{\overline{\theta}}{f_{\mathrm{PQ}}/N} \frac{2z}{(1+z)^2} \langle N|\sigma|N\rangle \approx 0.03 \frac{\overline{\theta} m_N}{f_{\mathrm{PQ}}/N},$$

where $\langle N|\sigma|N\rangle = 60$ MeV is a pion-nucleon coupling term from the current algebra, $z = 0.63$ is the ratio of the up and down quark masses, and $\overline{\theta}$ is the coefficient of the induced scalar couplings of the axion [12,13]. Combining these expressions we predict

$$(g_s g_p)_e = (g_{aNN})_s (g_{aee})_p = 0.18 \frac{\overline{\theta} m_N m_e}{(f_{\mathrm{PQ}})^2}$$

and

$$(g_s g_p)_n = (g_{aNN})_s (g_{ann})_p = 0.086 \frac{\overline{\theta} m_N m_n}{(f_{\mathrm{PQ}})^2}.$$

The Peccei-Quinn symmetry breaking scale is related to the range through the expression $\lambda_a = (0.5\ \mathrm{cm})[f_{\mathrm{PQ}}/(10^{12}\ \mathrm{GeV})]$. Neutron electric-dipole measurements [14], together with theory [15], place upper bounds on $\overline{\theta}$ of about 4×10^{-10}. The values predicted by the axion models for various ranges and values of $\overline{\theta}$ are shown in Fig. 3. It should be kept in mind that the predictions for the electron represent a model-dependent upper bound. The present results are about 4 orders of magnitude closer to the theoretical predictions for the neutron than they are for the maximal electron prediction. Because Hg is so much more sensitive to an axion coupling, it is essentially the axion sensor in our experiment, while the Cs oscillator allows us to remove magnetic fluctuations. The limit obtained for coupling to the neutron spin is far more sensitive to the monopole-dipole axion coupling than all previous experiments. Unfortunately, the results are still several orders of magnitude too large to further restrict the axion window from its present range.

Extension of the present results to shorter ranges could be accomplished through the introduction of a large movable mass closer to the experimental cells. This could be achieved using high purity liquid Hg in a closed, nonmagnetic but conductive chamber inside the magnetic shields. The modulation of the Hg mass position could be accomplished simply by pressurizing and depressurizing appropriate parts of the chamber. Our apparatus could also be used to search for a spin-spin coupling by replacing the lead masses with an appropriately prepared material, such as Dy_6Fe_{23}, which has a net electronic spin but no net magnetic moment [16].

We wish to thank Hyunji Cho for assistance with the planning of the experiment, Leslie Rosenberg for helpful conversations, and Donald Martin, Phillip Grant, and Robert Bartos for technical assistance. This work was supported by NSF RUI Grant No. PHY-9402701 and an Amherst College faculty research award. S.K.L. was supported by NSF Grant No. PHY-9206408.

[1] E. W. Kolb and M. S. Turner, *The Early Universe* (Addison-Wesley, Redwood, CA, 1990).
[2] J. E. Moody and F. Wilczek, Phys. Rev. D **30**, 130 (1984).
[3] L. J. Rosenberg, in *Proceedings of the Workshop on Particle and Nuclear Astrophysics in the Next Millennium, Snowmass* (World Scientific, Singapore, 1994).
[4] D. J. Wineland, J. J. Bolinger, D. J. Heinzen, W. M. Itano, and M. G. Raizen, Phys. Rev. Lett. **67**, 1735 (1991).
[5] B. J. Venema, P. K. Majumder, S. K. Lamoreaux, B. R. Heckel, and E. N. Fortson, Phys. Rev. Lett. **68**, 135 (1992).
[6] R. C. Ritter, L. I. Winkler, and G. T. Gillies, Phys. Rev. Lett. **70**, 701 (1993).
[7] C. J. Berglund, L. R. Hunter, D. Krause, Jr., E. O. Prigge, and M. S. Ronfeldt, Phys. Rev. Lett. **75**, 1879 (1995).
[8] Because of the construction of a new wing on the science building, data could not be collected during the week when the laboratory magnetic field would abruptly jump by 0.3 mG every time an arc welder was turned on or off.
[9] Chauvenet's criterion is essentially that a data point is suspect if the probability of obtaining one such point in a random sample of N data points is less than 50%. cf. John R. Taylor, *An Introduction to Error Analysis* (University Science Books, Mill Valley, CA, 1982).
[10] J. P. Jacobs, W. M. Klipstein, S. K. Lamoreaux, B. R. Heckel, and E. N. Fortson, Phys. Rev. Lett. **68**, 135 (1992).
[11] R. C. Ritter (private communication).
[12] J. E. Kim, Phys. Rep. **150**, 1 (1987).
[13] R. Barbieri, R. N. Mohapatra, D. V. Nanopoulos, and D. Wyler, Phys. Lett. **107B**, 80 (1981).
[14] I. S. Altrarev *et al.*, Phys. Lett. B **267**, 242 (1992); K. F. Smith *et al.*, Phys. Lett. B **237**, 191 (1990).
[15] V. Baluni, Phys. Rev. D **9**, 2227 (1979); R. J. Crewther, P. Di Vecchia, G. Veneziano, E. Witten, Phys. Lett. **88B**, 123 (1979); Phys. Lett. **91B**, 487(E) (1980).
[16] R. C. Ritter, C. E. Goldblum, W.-T. Ni, G. T. Gillies, and C. C. Speake, Phys. Rev. D **42**, 977 (1990).